

Coupling between SW monsoon-related surface and deep ocean processes as discerned from continuous particle flux measurements and correlated satellite data

T. Rixen, B. Haake, and V. Ittekkot

Institut für Biogeochemie und Meereschemie, Universität Hamburg, Hamburg, Germany

M.V.S. Guptha and R.R. Nair

National Institute of Oceanography, Goa, India

P. Schlüssel

Meteorologisches Institut, Ludwig-Maximilian-Universität München, Munich, Germany

Abstract. Particle flux data obtained by time series sediment traps deployed at water depths of approximately 3000 m in the western, central, and eastern Arabian Sea since 1986 were compared with wind speeds derived from measurements made by microwave radiometer flying on polar orbiting satellites and sea surface temperatures (SSTs) provided by the Physical Oceanography Distributed Active Archive Center at Jet Propulsion Laboratory. This comparison has allowed us to trace the link between the oceanographic and biological processes related to the development of the SW monsoon with the pattern and interannual variability of particle fluxes to the interior of the Arabian Sea. We could recognize the well-known upwelling systems along the coasts of Somalia and Oman as well as open ocean upwelling at the beginning of the SW monsoon. Both open ocean upwelling and coastal upwelling off Oman cause a cooling of surface waters at our western and central Arabian Sea stations. When SSTs fall below their long-term average, an increase in fluxes which are dominated by coccolithophorid-derived carbonates occurs. The timing of this increase is determined by the rate of surface water cooling. Further intensification of upwelling as the SW monsoon progresses causes additional increases in biogenic opal fluxes denoting diatom blooms in the overlying waters. The total fluxes during this period are the highest measured in the open Arabian Sea. At the central Arabian Sea location the fluxes are only randomly affected by these blooms. The particle flux in the eastern Arabian Sea is as high as in the central Arabian Sea but is influenced by a weaker upwelling system along the Indian coast. The observed interannual variability in the pattern of particle fluxes during the SW monsoons is most pronounced in the western Arabian Sea. This is controlled by the intensity of the upwelling systems on the one hand and the transport of cold, nutrient-poor, south equatorial water into the Oman region on the other. The latter effect, which is strongest during the SW monsoon with highest recorded wind speeds, reduces the influence of upwelling and the related particle fluxes at the western Arabian Sea station, where highest fluxes occur during SW monsoons with moderate wind speeds. Thus coastal and open ocean upwelling are most effective in transferring biogenic matter to the deep sea during the SW monsoons of intermediate strength.

1. Introduction

1.1. Monsoon

The Arabian Sea is strongly influenced by the Asian monsoons. The monsoon system is driven by the atmospheric

pressure difference between land and ocean. Boreal cooling of the land mass during winter and heating during summer result in high and low atmospheric pressure over Asia. The reverse, atmospheric lows during winter and atmospheric highs during summer, occurs over the Indian Ocean. The geostrophically balanced air flow results in strong, topographically steered (East African and Makran Highlands) SW winds during summer (SW monsoon) and moderate NE winds during winter (NE monsoon) [e.g., Findlater, 1969; Ramage, 1971, 1987; Tchernia, 1980].

Copyright 1996 by the American Geophysical Union.

Paper number 96JC02420.
0148-0227/96/96JC02420\$09.00

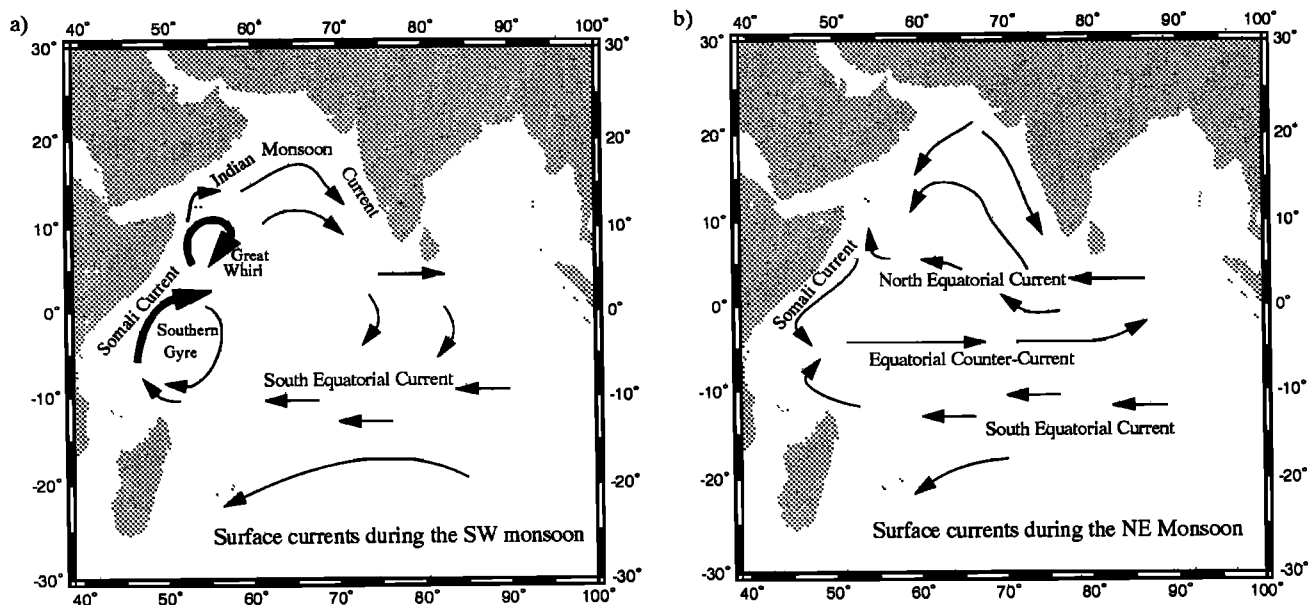


Figure 1. Surface currents in the Indian Ocean during the (a) SW and, (b) NE monsoons (information from Molinari et al. [1990], Wyrki [1973], Bearmann et al. [1989], and Fischer et al. [1996]).

Furthermore, the extreme atmospheric low during the SW monsoon over south west Asia diverts the southern hemisphere trade winds to cross the equator between 38°E and 55°E [Findlater, 1969; Tchernia, 1980]. This results in the formation of the Findlater Jet, an approximately 200 - 400 km wide area of strong wind stress almost parallel to the Arabian Peninsula over the Arabian Sea [Findlater, 1966, 1969; Legler et al., 1989].

1.2. Upper Ocean Response

The reversal of wind direction enforces a drastic change of surface ocean currents in the western equatorial Indian Ocean and the Arabian Sea. The anticlockwise surface circulation during the NE monsoon gets replaced by the clockwise flowing Indian Monsoon Current during the SW monsoon [Tchernia, 1980] (Figure 1). Similarly, the Somali current reverses between the NE and SW monsoon to a northward flow into the Arabian Sea during the SW monsoon [Wyrki, 1973]. During this season the Somali current consists of two gyres, the Southern Gyre and the Great Whirl. Surface current velocities of up to 4 m s⁻¹ were reported within these gyres [Düing et al., 1980; Swallow, 1981; Evans and Brown, 1981; Schott, 1983]. The cross-equatorial transport into the Arabian Sea was estimated to be $13 \times 10^6 \text{ m}^3 \text{ s}^{-1}$ in the surface layer of the Somali current [Schott, 1983; Schott and Fieux, 1985]. Associated with the Somali current and due to the prevailing wind directions, upwelling appears north of the two gyres and between the Somali current and the coast [Brown et al., 1980; Evans and Brown, 1981; Schott, 1983; Tsai et al., 1992]. Off Oman, an upwelling area extending approximately 700 km offshore is generated by coastal upwelling [Sastry and D'Souza, 1972; Bruce, 1974] merging with open ocean upwelling which develops beneath the Findlater Jet [Luther et al., 1990; Brock et al., 1991]. A weaker upwelling takes place along the coast of India [Sharma, 1978; Shetye et al., 1990].

The seasonal appearance of upwelling is responsible for the high primary production in the Arabian Sea [Ryther and Menzel, 1965; Ryther et al., 1966; Qasim, 1977; Berger et al., 1988]. These extreme, wind-driven seasonal changes of upper ocean

physical and biological processes make the Arabian Sea an ideal area to study climatic effects on the amount of particles settling to the deep sea.

1.3. Particle Fluxes

First results from our ongoing time series sediment trap experiments in the western, central, and eastern Arabian Sea since 1986 (Figure 2) have shown that the particle flux to the deep Arabian Sea is strongly influenced by the monsoons [Nair et al., 1989]. It was suggested that higher wind speeds during the SW monsoon result in a more intense upwelling causing enhanced particle fluxes into the deep sea [Haake et al., 1993b]. Deviations from this trend were explained by a northward shift of the Findlater Jet, which results in a reduced open ocean upwelling at the trap location in the western Arabian Sea [Dube et al., 1990; Anderson and Prell, 1992; Haake et al., 1993a].

We have extended these investigations by including in the interpretation of particle fluxes, data on wind speeds from a satellite-carried microwave radiometer (special sensor microwave imager (SSM/I)) between 1986 and 1992 and the sea surface temperature response to monsoon winds derived from the advanced very high resolution radiometer (AVHRR), provided by the Physical Oceanography Distributed Active Archive Center at Jet Propulsion Laboratory, California Institute of Technology. This has allowed us to resolve the link between the development of the monsoons over the western Indian Ocean and the material flux into the interior of the Arabian Sea.

2. Methods

Three moorings, each consisting of a Mark VI time series sediment trap [Honjo and Doherty, 1988] at approximately 3000-m water depth, have been deployed in the western, central, and eastern Arabian Sea since 1986 (Figure 2, Table 1). Sampling intervals were between 12 and 27 days. Prior to deployment the sampling cups were filled with seawater from the deep Arabian Sea to which sodium chloride (35 g NaCl L⁻¹) and mercury(II)-

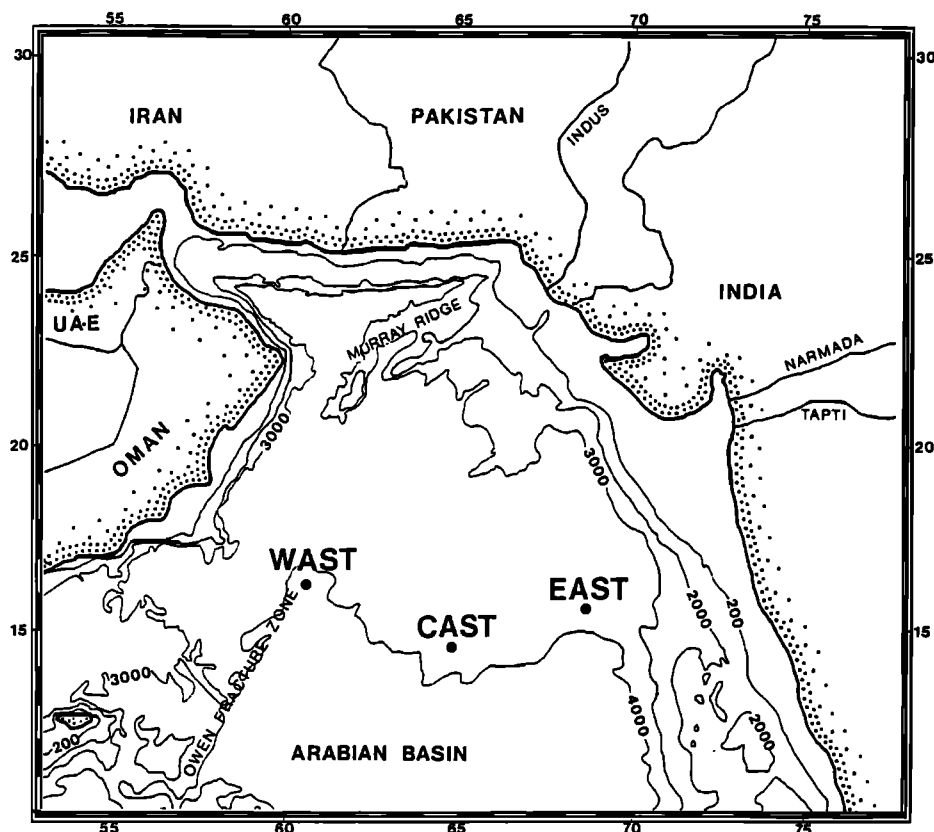


Figure 2. Sediment trap locations in western (WAST), central (CAST), and eastern (EAST) Arabian Sea.

chloride (3.3 g L^{-1}) were added to prevent the degradation of trapped material.

After recovery, the supernatant was decanted and the residue was wet sieved using a 1-mm sieve. The $< 1\text{-mm}$ fraction was split into aliquots, filtered through preweighted $0.4\text{-}\mu\text{m}$ polycarbonate membrane filters (Nucleopore), and dried at 45°C . Total flux was calculated using the filtered material. The $>1\text{-mm}$ fraction was not included in the calculations of total fluxes [Honjo, 1982; Lee *et al.*, 1988]. The accuracy of fluxes measured by sediment traps has the potential to be affected by hydrodynamic biases and by the influence of swimmers [e.g., Gust *et al.*, 1992, 1994; Lee *et al.*, 1992]. Despite such limitations, the correlation between the monsoon-driven surface ocean processes and the flux measurements in 3000-m water depth as discussed by Nair *et al.* [1989] and Haake *et al.* [1993a, b] reveals that sediment traps deployed in the deep-sea record sequences of environmental events in the surface layer and allow a continuous and quantitative determination of matter sinking from the surface ocean to the underlying sediments. Samples affected by malfunctioning of the traps and by swimmers are not included in the following discussion.

2.1. Chemical Analysis of Sediment Trap Samples

Carbonate was determined with a Charnograph 6 (Wösthoff). The sample was heated in 2 N phosphoric acid and the released carbon dioxide passed through a 0.05 N sodium hydroxide solution. Carbonate concentrations were calculated from the conductivity changes of the sodium hydroxide solution. Pure carbonate was used for calibration. Reproducibility of this method is $\pm 1\%$.

Total carbon and total nitrogen were measured with a Carlo Erba Nitrogen Analyser 1500. After sample combustion, carbon, as carbon dioxide, and nitrogen were detected in a constant helium flow by a heat conductivity detector. Reproducibility of this method is 0.02% for carbon and 0.05% for nitrogen. Organic carbon was determined as the difference between carbonate carbon and total carbon. Organic matter was calculated by multiplying organic carbon by 1.8 [Müller *et al.*, 1986].

Biogenic opal determination was based on a method modified from Mortlock and Froelich [1989] and Koroleff [1983]. After removing the carbonate by adding 2 N hydrochloric acid and organic matter by adding hydrogen peroxide (2%), the remaining sample was heated for 5 hours with sodium carbonate (7%) for leaching biogenic silicon which was subsequently detected photometrically. To obtain the biogenic opal concentration, the silicon concentration was multiplied with 2.4 [Mortlock and Froelich, 1989]. The reproducibility of this method is 1% biogenic opal. Total biogenic matter was calculated as the sum of biogenic opal, carbonate, and organic matter.

2.2. Satellite Data

Weekly averaged wind speeds were derived from SSM/I measurements from July 1987 to December 1992 by using an algorithm developed by Schlüssel [1995]. Accuracy of the method is 1.4 m s^{-1} . Additional wind speeds were obtained from ship observations (Indian Daily Weather Report, Pune) at the trap locations between July 1987 and October 1990. These wind speeds are higher approximately by a factor of 1.6 than the satellite data with which they are well correlated ($r^2 = 0.678$). Since satellite-derived wind speeds are not available between 1986 and

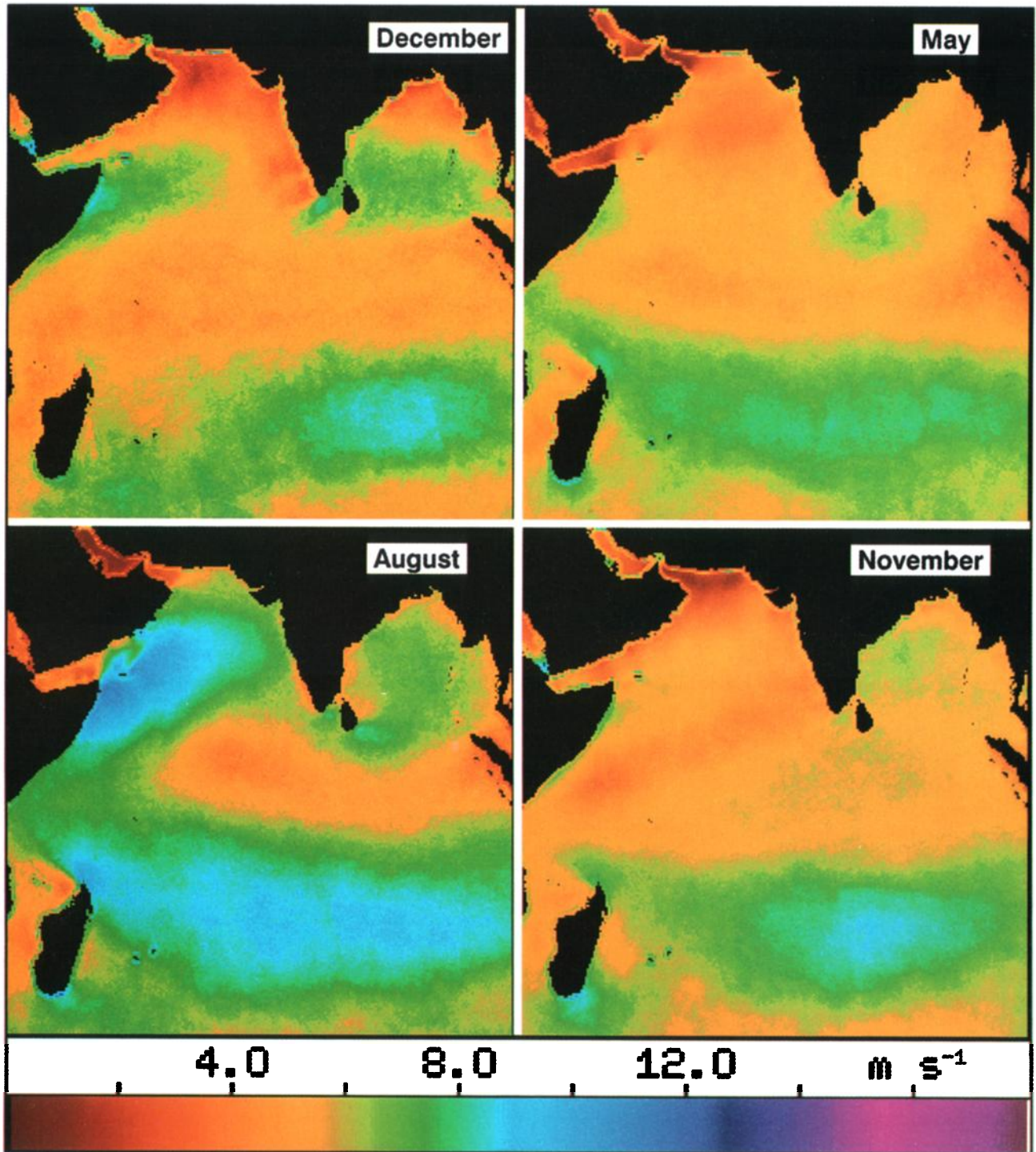


Plate 1. Mean wind speeds during the NE monsoon in December, during the SW monsoon in August, and during the intermonsoons in May and November (averaged over the period of observation).

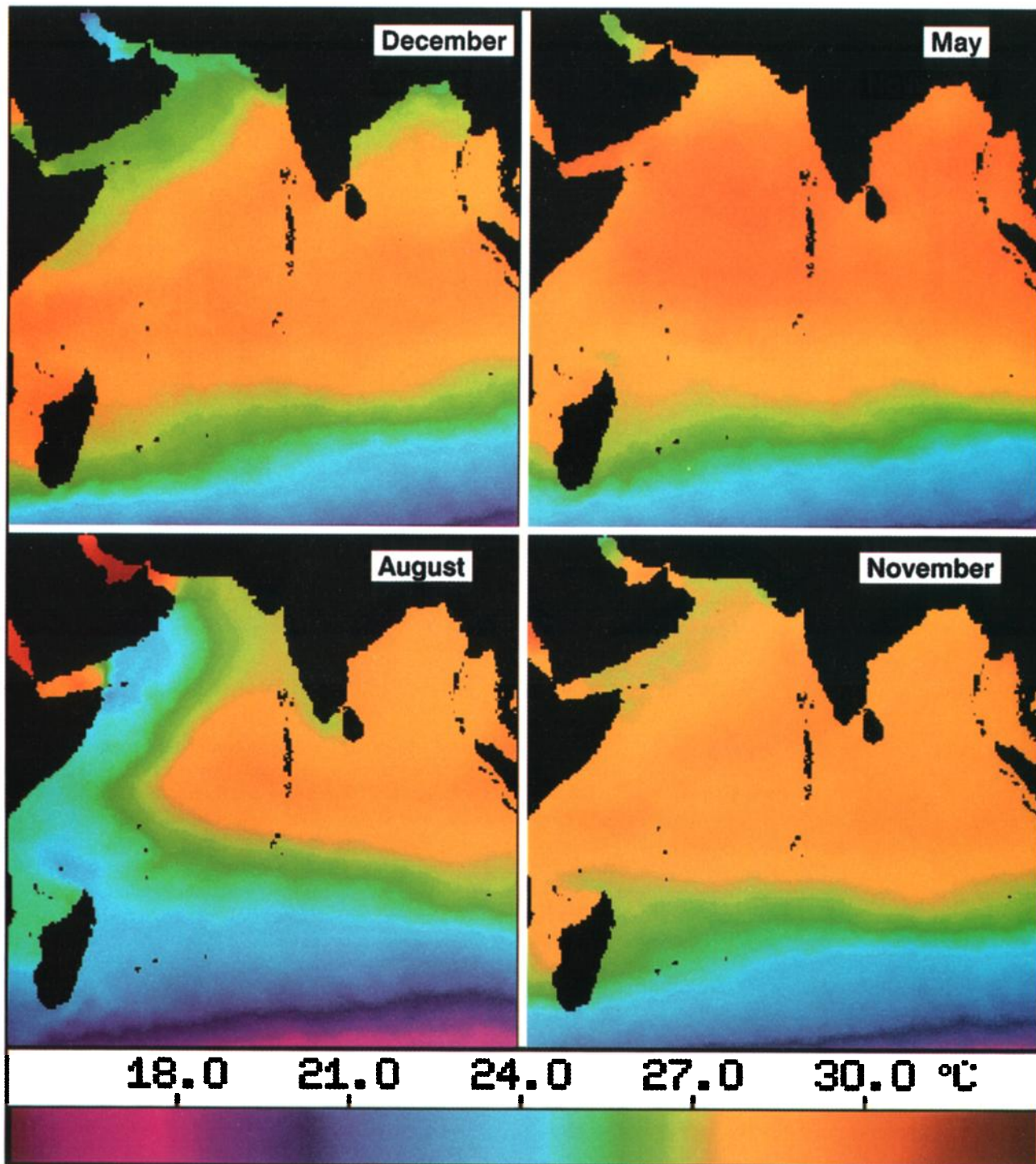


Plate 2. Mean sea surface temperatures during the NE monsoon in December, during the SW monsoon in August, and during the intermonsoons in May and November (averaged over the period of observation).

Table 1. Stations, Locations, Trap Depths, Water Depths at Trap Locations, Deployment Periods, and Sampling Intervals

Station	Position	Trap Depth, m	Water Depth, m	Deployment Period		Interval, days
				Start	End	
Wast-01	16° 23' N 60°32'E	3024	4020	May 10, 1986	Oct. 26, 1986	13.0
Wast-02	16° 18' N 60°28'E	3021	4018	Nov. 19, 1986	May 1, 1987	12.6
Wast-03	16° 19' N 60°28'E	3033	4010	May 12, 1987	Oct. 21, 1987	12.5
Wast-04	16° 35' N 60°28'E	3039	4016	Nov. 22, 1987	Oct. 31, 1988	26.5
Wast-05	16° 24' N 60°29'E	3029	4016	Nov. 20, 1988	Sept. 28, 1989	24.0
Wast-06	16° 19' N 60°31'E	3016	4013	Jan. 15, 1990	Oct. 15, 1990	21.0
Wast-07	16° 20' N 60°32'E	3039	4027	Dec. 19, 1990	Oct. 26, 1991	25.0
Wast-08	16° 19' N 60°30'E	3030	4018	Jan. 16, 1992	Dec. 16, 1992	26.0
Cast-01	14° 32' N 64°44'E	2919	3900	May 10, 1986	Oct. 26, 1986	13.0
Cast-02	14° 29' N 64°46'E	2894	3912	Nov. 19, 1986	May 1, 1987	12.6
Cast-03	14° 28' N 64°46'E	2913	3890	May 12, 1987	Oct. 21, 1987	12.5
Cast-04	14° 33' N 64°47'E	2933	3910	Nov. 22, 1987	Oct. 31, 1988	26.5
Cast-05	14° 36' N 64°50'E	3109	3906	Nov. 20, 1988	Sept. 28, 1989	24.0
Cast-06	14° 35' N 64°47'E	3011	3950	March 29, 1990	Nov. 23, 1990	21.0
Cast-07	14° 35' N 64°46'E	2884	3921	Dec. 19, 1990	Oct. 26, 1991	25.0
Cast-08	14° 34' N 64°45'E	2876	3913	Jan. 19, 1992	Dec. 16, 1992	26.0
East-01	15° 32' N 68°45'E	2787	3370	May 10, 1986	Oct. 26, 1986	13.0
East-02	15° 28' N 68°45'E	2764	3782	Nov. 19, 1986	May 1, 1987	12.6
East-03	15° 26' N 68°43'E	2773	3770	May 12, 1987	Oct. 21, 1987	12.5
East-04	15° 32' N 68°45'E	2778	3775	Nov. 22, 1987	Oct. 31, 1988	26.5
East-05	15° 15' N 68°36'E	2947	3751	Nov. 20, 1988	Sept. 28, 1989	24.0
East-06	15° 38' N 68°34'E	2928	3862	Nov. 27, 1990	Nov. 23, 1990	21.0
East-07	15° 37' N 68°33'E	2952	3828	Dec. 19, 1990	Oct. 26, 1991	25.0

July 1987, wind speeds from ship observations multiplied by 0.6 were used for this period.

Weekly composites, 18 km x 18 km gridded, day and night, multichannel sea surface temperatures (SST) were provided by the Physical Oceanography Distributed Active Archive Center at Jet Propulsion Laboratory, California Institute of Technology. The accuracy of the SST is better than 1°K [McMillin and Crosby, 1984; McClain et al., 1985]. Further, the night and day SSTs were averaged and interpolated of the SSM/I grid (0.25 degrees). For comparison of satellite and particle flux data, the satellite data were averaged within a radius of 1 degree around the sediment trap locations, and all data were interpolated for the same biweekly intervals.

For discussion of the interannual variability the enhanced particle flux rates within the SW monsoon were averaged. Mean SW monsoon wind speeds and SSTs were averaged taking into account a delay of approximately 14 days between surface ocean processes and particle fluxes in the deep sea.

3. Results and Discussion

3.1. Wind Speeds and Sea Surface Temperatures

Plates 1 and 2 depict the seasonal changes of wind speeds and SSTs over the northern Indian Ocean. The following general features can be discerned: Wind speeds are low during the intermonsoon and rise considerably during the SW monsoon. Sea surface temperatures are high during the intermonsoon and low

during the SW monsoon, especially along the coasts of Somalia and Oman which can be attributed mainly to upwelling [Düing and Leetmaa, 1980; McCreary and Kundu, 1988].

During the SW monsoon the lowest SSTs occur within the upwelling center along the coasts of Somalia and Oman. Winter cooling during the NE monsoon results in lowest SSTs in the northernmost Arabian Sea. The onset of upwelling is defined by the first appearance of cold surface water in the upwelling regions off Somalia and Oman at the beginning of the SW monsoon in May or June. The following discussion will focus first on the western and central Arabian Sea influenced by these upwelling systems followed by the eastern Arabian Sea, which is affected by a different system.

3.2. Western and Central Arabian Sea

3.2.1. Total flux. The seasonal variation of the particle fluxes in the western, central, and eastern Arabian Sea shows a bimodal pattern with high fluxes during the SW and NE monsoons (Figure 3). These enhanced fluxes during the SW and NE monsoons are almost on the same level at all three sediment trap stations except for the SW monsoon fluxes at the western station located underneath the Findlater Jet, within the upwelling area off Oman. At the western Arabian Sea site, the fluxes are more than twice as high as in the central and eastern Arabian Sea during the SW monsoon and are among the highest recorded worldwide [e.g., Deuser et al., 1981; Honjo, 1982; Dymond and Collier, 1988; Wefer et al., 1988; Wefer, 1989; Wefer and Fischer, 1993]. These

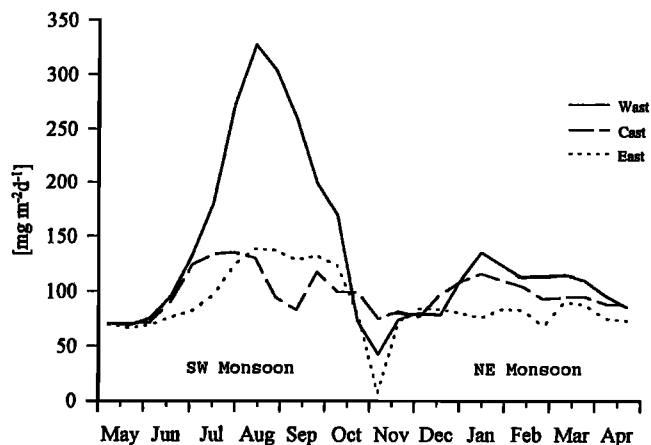


Figure 3. Total fluxes at the western (Wast), central (Cast), and eastern (East) Arabian Sea stations averaged over the whole period of observation.

fluxes consist of up to 36% biogenic opal mostly in the form of *Rhizosolenia sp.* and *Nitzschia sp.* and of up to 57% carbonate, dominated by the foraminifera *Globigerina bulloides* [Curry et al., 1992]. These well-known upwelling species confirm the link between upwelling and enhanced particle fluxes to the deep sea.

The onset of upwelling in the western Arabian Sea occurs following the variation of the wind field with the opening of the SW monsoon between beginning of May and June. At this time the wind speeds rise beyond their long-term average in the western (Figure 4) and central Arabian Sea (Figure 5); decreasing SSTs mark the upwelling influence at both stations approximately 1 week later. With the SST drop below its long-term average, particle fluxes at 3000-m depth start to increase at the western and central Arabian Sea stations (Figures 4 and 5). The delay between the onset of upwelling and the increase of particle fluxes at 3000-m water depth at these sites varies between 2 to 8 weeks and depends on the rate of cooling of surface water during this time, with a more rapid cooling of surface water leading to a shorter delay (Figure 6).

The shortest delay of 14 days between the onset of upwelling and the increase of particle fluxes at both stations was registered in the beginning of the 1987 SW monsoon (Figure 6). SST charts for this period indicate a cooling of surface water from the coast of Somalia toward the sediment trap stations in the central and western Arabian Sea within a week which might be interpreted as a result of lateral advection of cold upwelled water (Figure 7b). The available information as assessed from drift buoy experiments shows a mean advection velocity of surface water of about 0.2 m s^{-1} (D. Quadfasel, personal communication, 1996) which is too low to explain the observed decreasing SST at the sediment

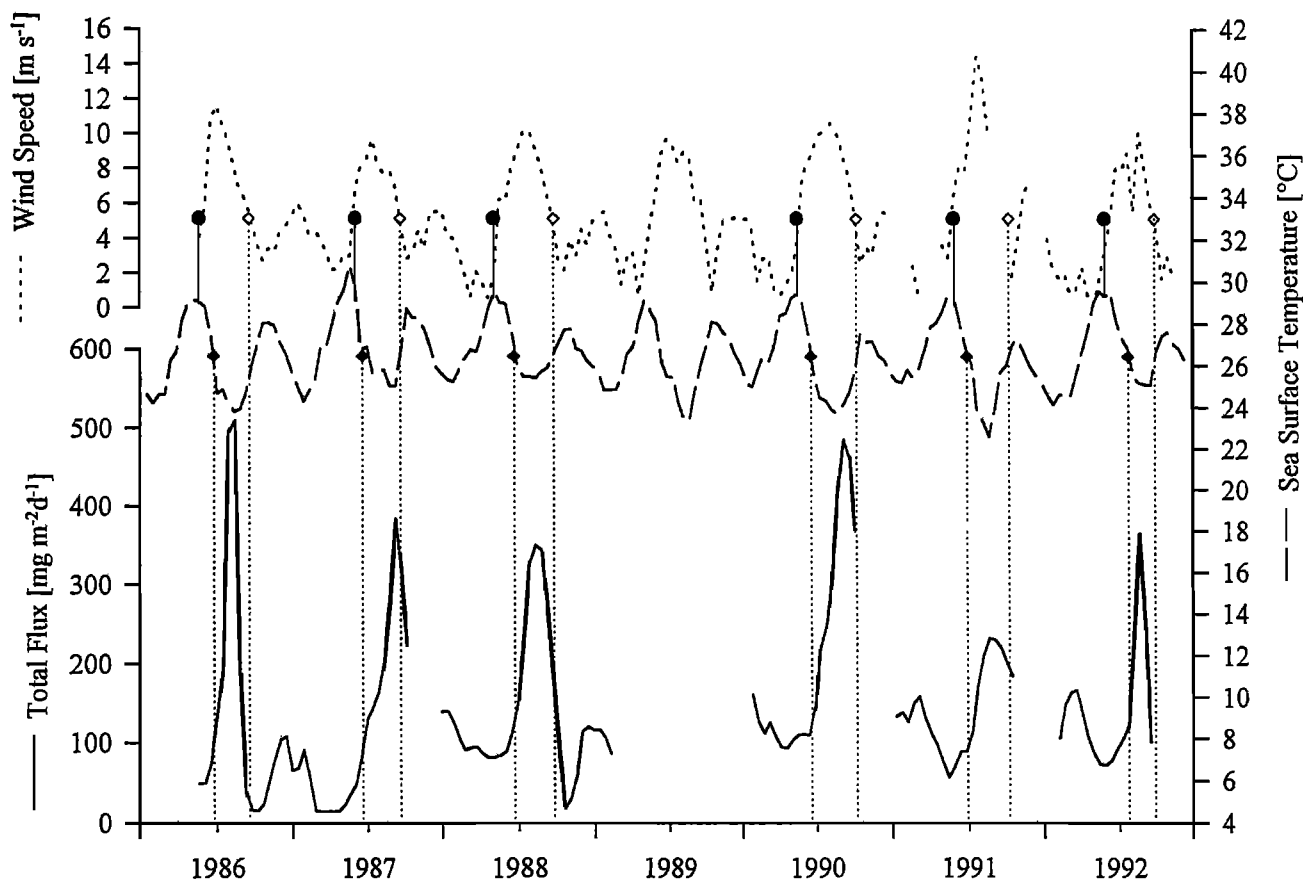


Figure 4. Wind speeds, sea surface temperatures, and total fluxes at the western Arabian Sea station. Solid circles mark the time in May/June each year when upwelling starts, surface water begins to cool, and wind speeds rise beyond the long-term average. Solid diamonds show the time when sea surface temperatures decrease below the long-term average and when particle fluxes at 3000-m water depth start to increase. Open diamonds mark the time when wind speeds fall below the long-term average, sea surface temperatures increase above the long-term average, and particle fluxes start to decrease.

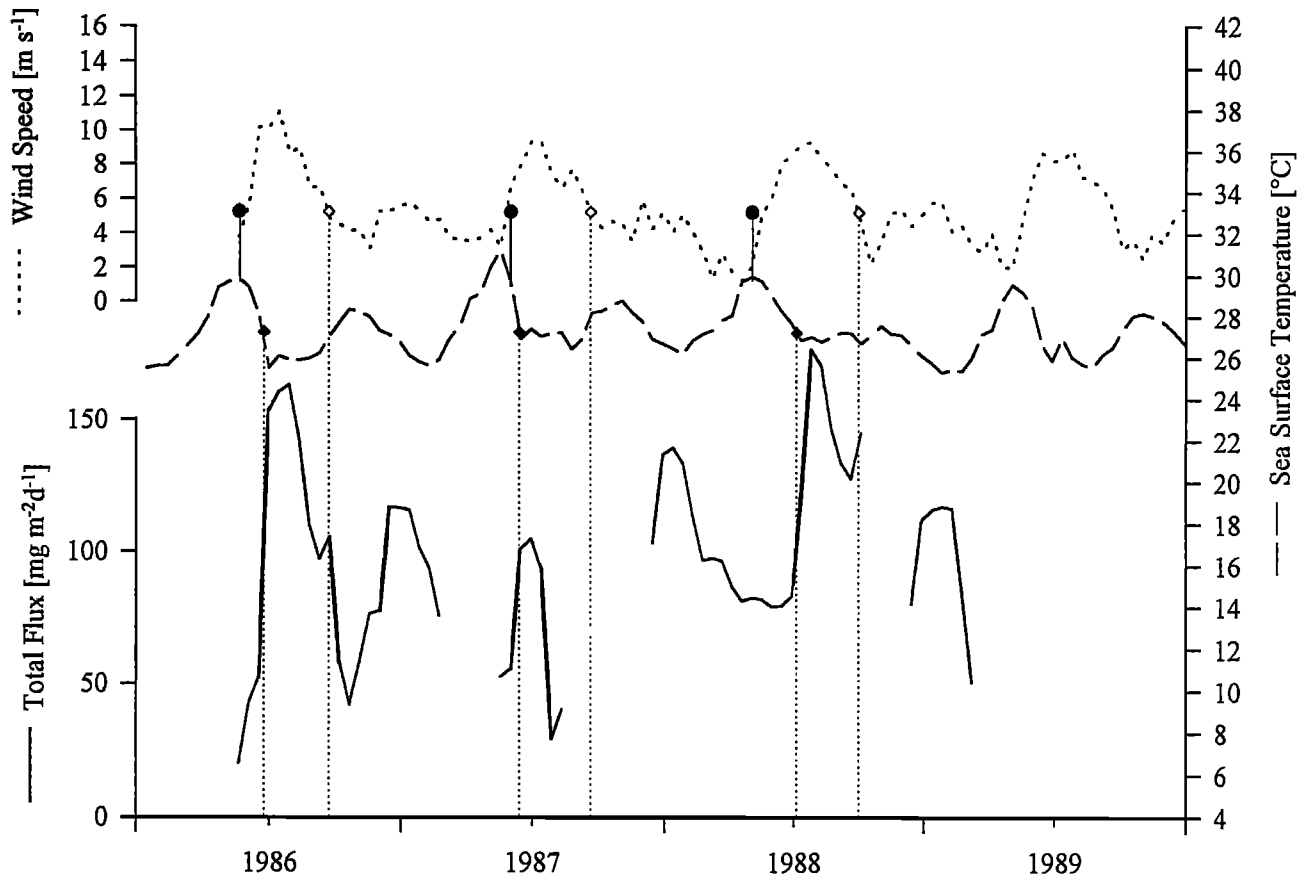


Figure 5. Wind speeds, sea surface temperatures, and total fluxes at the central Arabian Sea station. Solid circles mark the time in May/June each year when upwelling starts, surface water begins to cool, and wind speeds rise beyond the long-term average. Solid diamonds show the time when sea surface temperatures decrease below the long-term average and when particle fluxes at 3000-m water depth start to increase. Open diamonds mark the time when wind speeds fall below the long-term average, sea surface temperatures increase above the long-term average, and particle fluxes start to decrease.

trap positions by lateral advection alone. A similar observation could be made for the opening phase of the SW monsoon 1990, suggesting that at least during the years 1987 and 1990 the decreasing SSTs at the sediment trap station in the western and central Arabian Sea result mainly from local, open ocean

upwelling. The additional appearance of cold surface water along the Oman coast makes this feature of open ocean upwelling less distinct on SSTs charts during the other years and suggests the influence also of advected, upwelled water from the Oman coast on the particle flux in the western and central Arabian Sea (Figure 7a).

3.2.2. Carbonate and biogenic opal fluxes. Total flux in the Arabian Sea is dominated by carbonate derived from organisms such as coccolithophorids and foraminifera. Diatoms are important contributors to the biogenic opal flux, which is the second major component of the total flux. In the early phase of the SW monsoon, carbonate derived mainly from coccolithophorids increases, followed up to 8 weeks later by biogenic opal fluxes (Figure 8). Nutrient profiles obtained from the sediment trap locations before the onset of the SW monsoon reveal a steep increase of phosphate and nitrate concentrations just below the mixed layer at approximately 30-m water depth, whereas for silicate concentrations this occurs at about 150-m depth [Haake *et al.*, 1993a]. According to this nutrient distribution pattern, wind-induced mixed layer deepening at the beginning of the SW monsoon was suggested to be ineffective in injecting sufficient silicate into the euphotic zone to cause diatom blooms. Rather, the blooms resulted from upwelling [Haake *et al.*, 1993a]. Since upwelling is evident on SSTs charts already at the beginning of the SW monsoon, we assume that the silicate supply into the euphotic zone at the sediment trap location is controlled by the

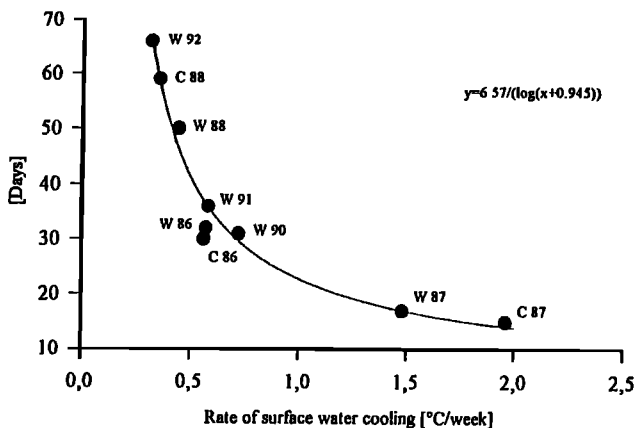


Figure 6. Lag between the onset of coastal upwelling and increase of particle flux at 3000-m water depth (y) plotted against the mean cooling velocity of surface waters per week (x) during the SW monsoons of 1986 to 1992 at the western (W86,..., W92) and central station (C86,..., C88).

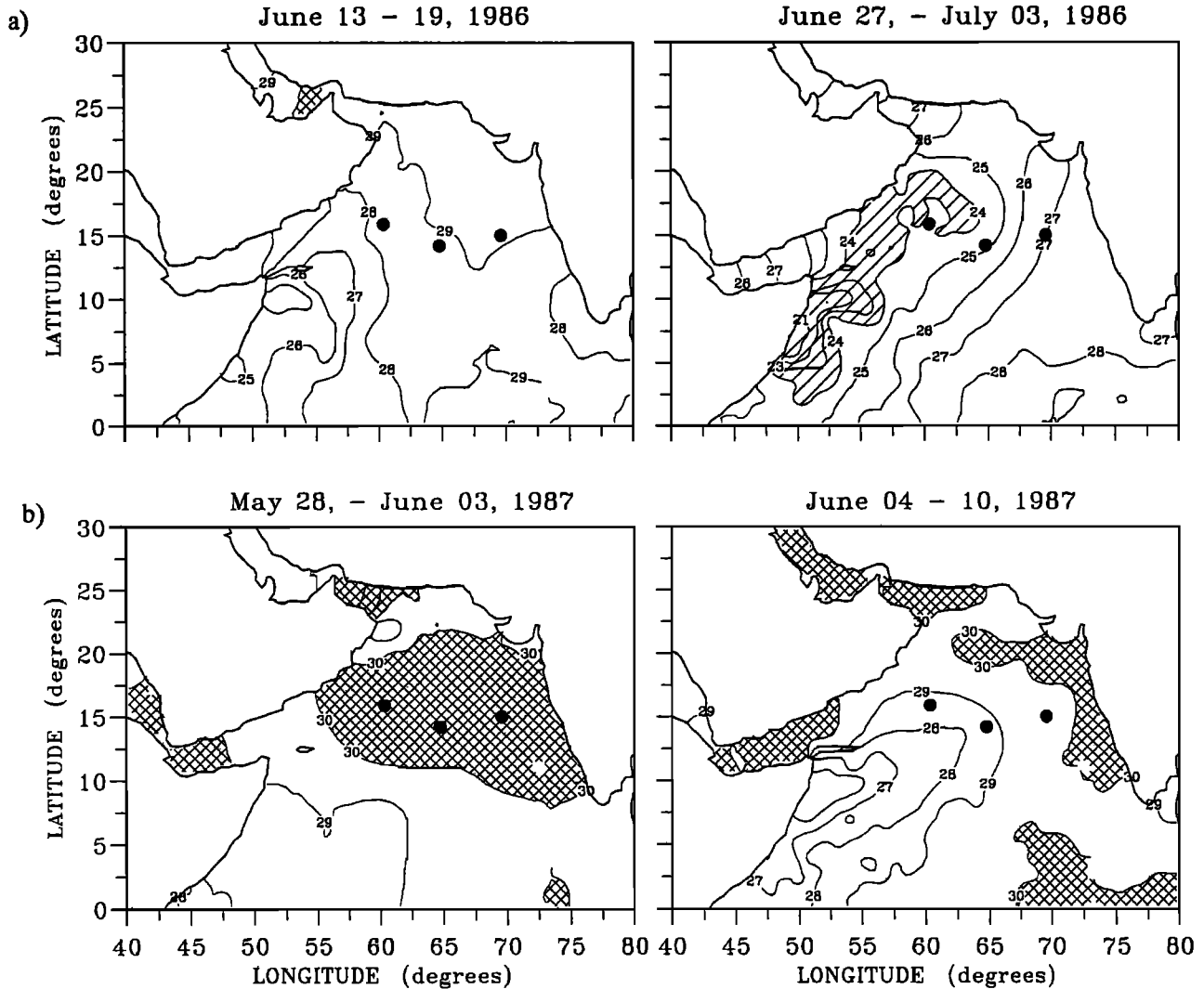


Figure 7. Weekly averaged sea surface temperatures during the onset of the SW monsoons in (a) 1986 and (b) 1987; cross hatching marks areas with sea surface temperatures of above 30°C and stripes indicate areas with sea surface temperatures below 24°C. Solid circles represent the sediment trap locations in the western, central, and eastern Arabian Sea.

intensity of open ocean upwelling and/or of advection of upwelled water from the Oman coast.

During the later phase of the SW monsoon a further decrease in SST indicates a stronger upwelling influence at the western Arabian Sea station. This is accompanied by peak fluxes of biogenic opal and organic matter. Satellite observations between 1979 and 1982 reveal plankton blooms covering the whole north-western Arabian Sea only within the later phase of the SW monsoon [Brock et al., 1991; Brock and McClain, 1992]. The occurrence of such blooms which were also related to both open ocean upwelling and advection of upwelled water from the Oman coast [Brock et al., 1991; Brock and McClain, 1992; Young and Kindle, 1994] seems to cause the high, diatom-related fluxes in the western Arabian Sea.

Total flux at the central Arabian Sea station reveals an increase similar to that at the western station during the early phase of the SW monsoon but does not reach the extreme peaks characteristic for the latter (Figure 3). According to the distribution of pigment concentrations [Brock et al., 1991; Brock and McClain, 1992], the central Arabian Sea station is at the edge of

the area affected by the extensive plankton blooms, and fluxes at this site seem to be only randomly influenced by these blooms.

3.2.3. Somali current. Mass sedimentation of material is a feature generally observed at the end of a diatom bloom during reduced nutrient availability [Degens and Ittekkot, 1984; Smetacek, 1985]. Average sinking speeds of marine particles range between 100 and 400 m day⁻¹ [Honjo and Roman, 1978; Alldredge and Silver, 1988], and it will take, approximately, 14 days for particles to sink from the surface to 3000-m water depth. However, in the western and central Arabian Sea, peak fluxes at 3000-m occur approximately simultaneously with minimum SST at the surface (Figures 4 and 5). This implies that cooling of surface water continues beyond the peak plankton bloom and points to a source of cold water other than upwelling.

Compared to the Arabian Sea, nutrient concentrations south of the equator are lower [Conkright et al., 1994]. The Somali current carries south equatorial water into the Arabian Sea [Düing et al., 1980; Swallow, 1981; Schott, 1983; Schott and Fieux, 1985] which flows between Somalia and Socotra into the upwelling regime off Oman [Fischer et al., 1996] and could play an impor-

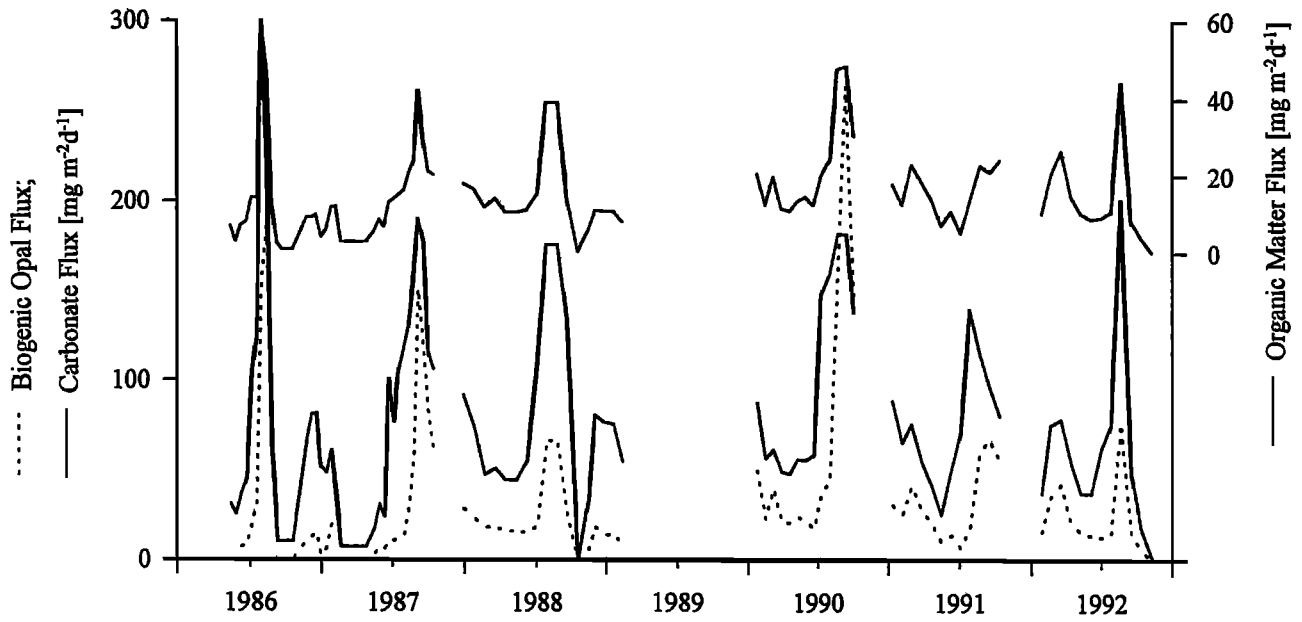


Figure 8. Flux rates of biogenic opal, carbonate, and organic matter at the western Arabian Sea Station.

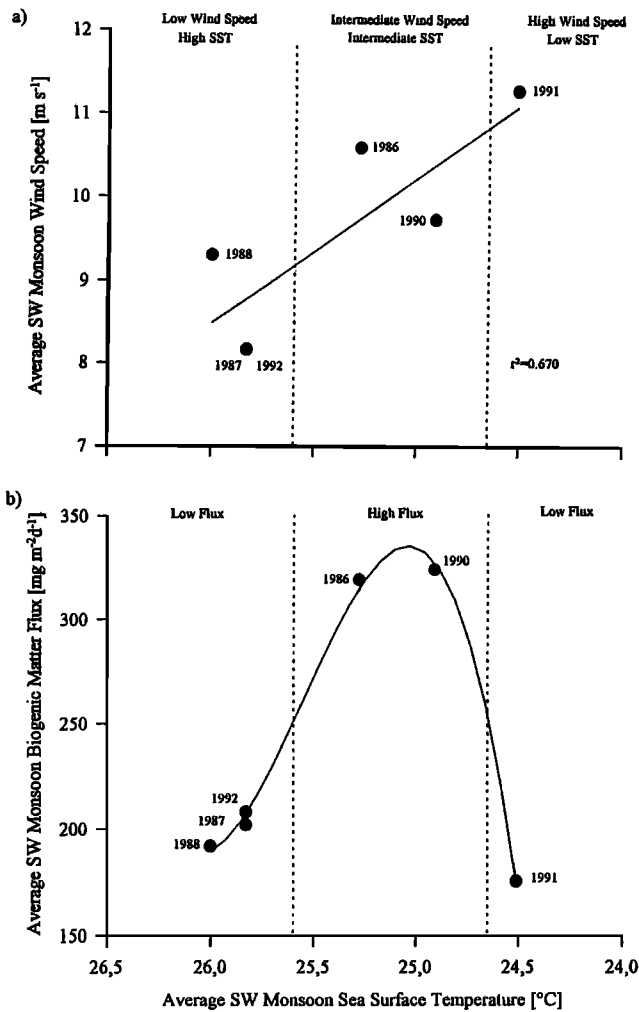


Figure 9. (a) Average SW monsoon wind speeds and (b) SW monsoon biogenic matter fluxes versus average SW monsoon sea surface temperatures.

tant role in controlling the nutrient regime within this area. The formation of a continuous boundary flow resulting from the collapse of the two gyre system of the Somali current in the later phase of the SW monsoon [Evans and Brown, 1981; Schott, 1983] could further enhance the cross-equatorial transport of nutrient-poor south equatorial water into the Arabian Sea. This process could determine the relationship between SST and particle fluxes.

3.2.4. Interannual variation of biogenic matter fluxes. The increase of particle fluxes and the appearance of peak fluxes in the western and central Arabian Sea varies by up to 4 weeks between the observed SW monsoons (1986-1992).

The average SW monsoon wind speeds range between 8 and 11 m s⁻¹ in the western Arabian Sea (Figure 9a). Higher average SW monsoon wind speeds lead to lower average SW monsoon

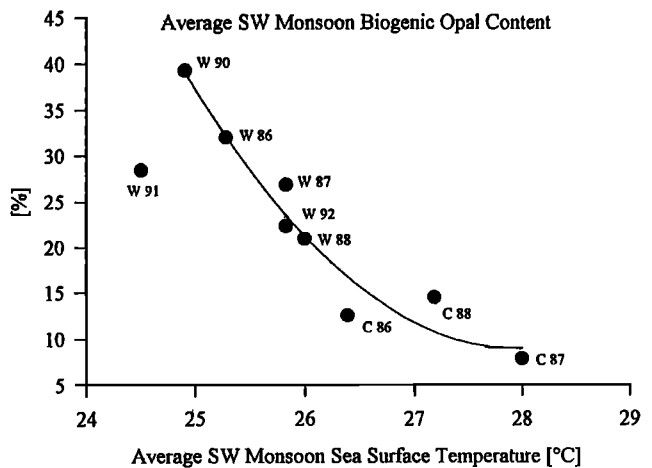


Figure 10. Average SW monsoons sea surface temperatures plotted against average SW monsoon biogenic opal contents (W, western; C, central Arabian Sea station; numbers represent the year). Solid curve shows second-order regression with $r^2 = 0.940$.

SST (Figure 9a). Lower values of SST are generally considered to be associated with enhanced nutrient concentrations [Smith, 1982; Brock et al., 1992] favoring diatom blooms and resulting in higher primary production and, subsequently, higher particle fluxes [Deuser and Ross, 1980; Deuser et al., 1981; Smetacek, 1985]. This is borne out by results from the western and central Arabian Sea which reveal lower SSTs corresponding with a higher contribution of diatoms to sinking matter as reflected by higher biogenic opal contents (Figure 10) and enhanced biogenic matter fluxes into the deep sea (Figure 9b). An exception to this general trend is the 1991 SW monsoon when the highest observed wind speeds and lowest SSTs are accompanied by the lowest biogenic matter fluxes in the western Arabian Sea (Figures 9a and 9b).

Average SSTs for the whole of the western Indian Ocean for the period of enhanced fluxes during the SW monsoons in 1986 to 1992 (Plate 3) reveal three distinct features: (1) a very pronounced propagation of cold surface water from the south into the Arabian during the SW monsoon 1991, (2) appearance of cold surface water along the coast of Somalia (SW monsoons in 1987, 1988, and 1992), and (3) additionally, appearance of cold surface water off Oman (SW monsoons in 1986 and 1990). The fluxes of biogenic matter are high during the SW monsoons with the third feature and low during the other SW monsoons. This shows that strong upwelling off Oman leads to high fluxes in the western

Arabian Sea. The low fluxes during the SW monsoon 1991 denote a weak upwelling, though SSTs indicate strong upwelling off Oman. Enhanced cross-equatorial transport of cold nutrient-poor surface water appears to reduce the influence of the Oman upwelling in the western Arabian Sea. Since highest average SW monsoon wind speeds are observed during the SW monsoon 1991 (Figure 9a), it could be assumed that this transport is reinforced by high wind speeds.

In the central Arabian Sea, high SSTs and low biogenic opal contents of the sinking matter (Figure 10) during the SW monsoon verify a weak influence of the upwelling-induced diatom blooms on particle flux compared to the western Arabian Sea. The interannual variations of SW monsoon fluxes are low and indicate that the observed variations of upwelling strength are insufficient to be clearly reflected in the particle flux observed in the central Arabian Sea.

3.3. Eastern Arabian Sea

Particle fluxes from the eastern Arabian Sea station do not correspond with the increase of wind speeds and the drop of SSTs in some of the years of investigation (Figure 11). Along the southwest coast of India, upwelling up to 15°N has been described [Sharma, 1978; Shetye et al., 1990]. Upwelling intensity is low compared to western Arabian Sea [Shetye et al., 1990] and cannot

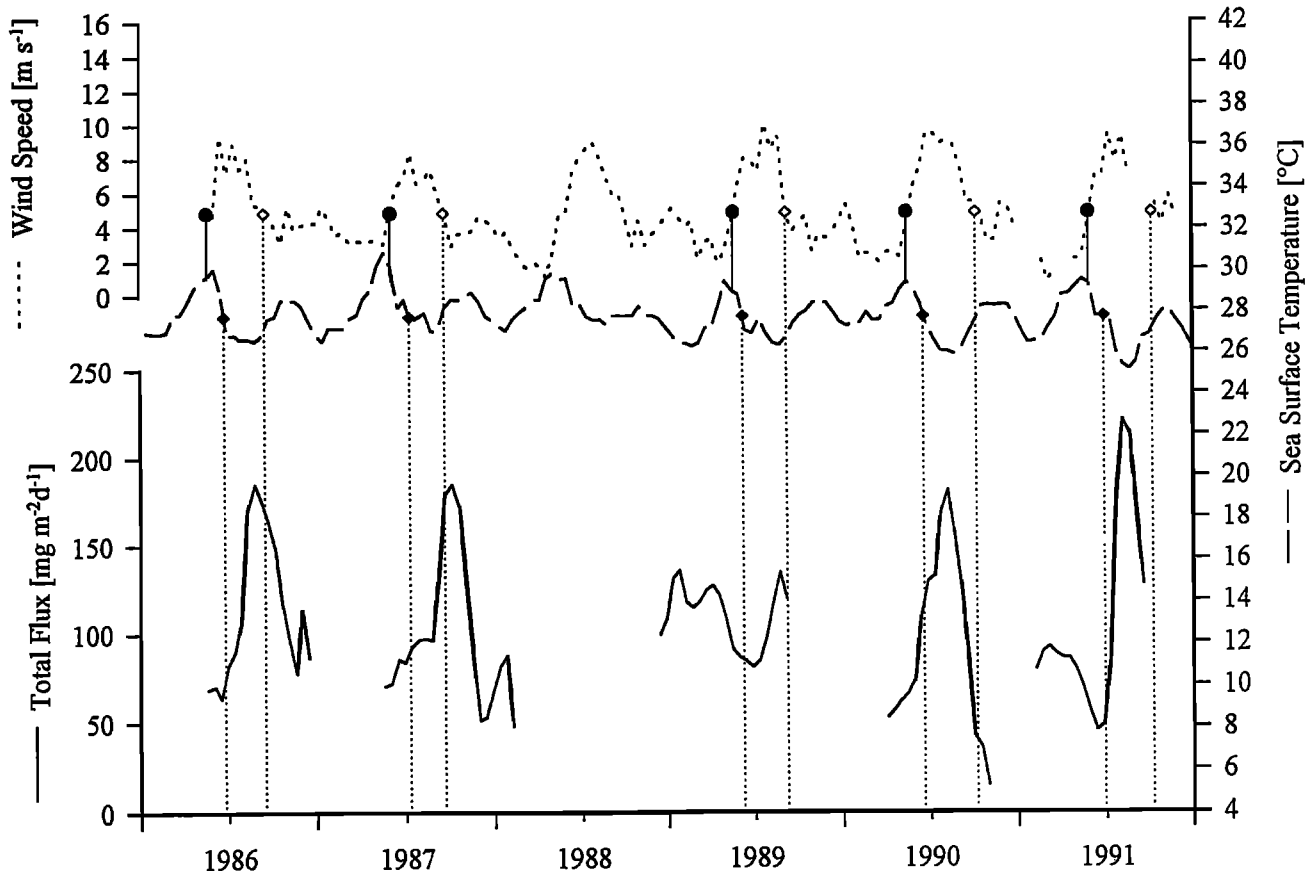


Figure 11. Wind speeds, sea surface temperatures, and total fluxes at the eastern Arabian Sea station. Solid circles mark the time in May/June each year when upwelling starts, surface water begins to cool, and wind speeds rise beyond the long-term average. Solid diamonds show the time when sea surface temperatures decrease below the long-term average and when particle fluxes at 3000-m water depth start to increase. Open diamonds mark the time when wind speeds fall below the long-term average, sea surface temperatures increase above the long-term average, and particle fluxes start to decrease.

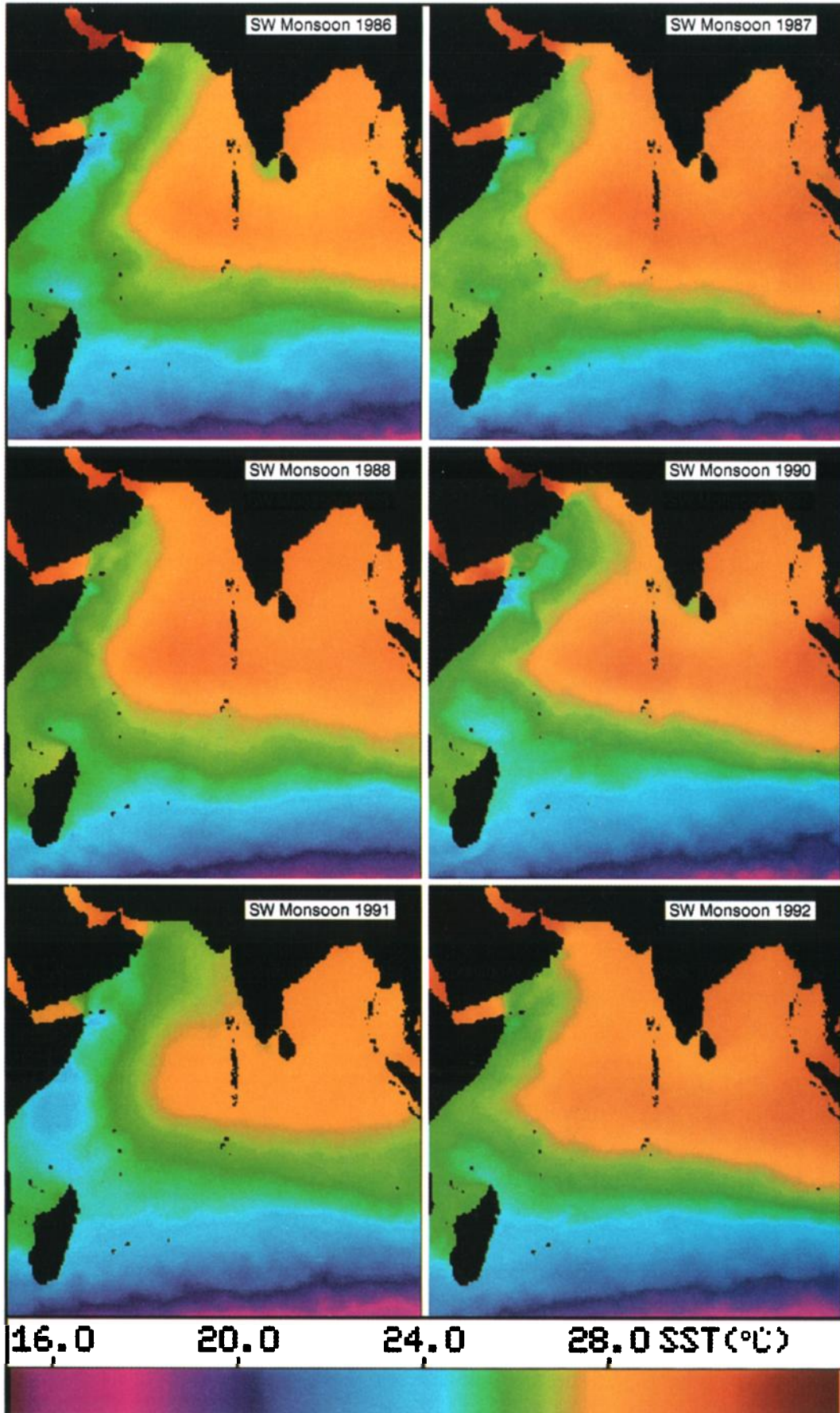


Plate 3. Average sea surface temperatures during the SW monsoons of 1986, 1987, 1988, 1990, 1991, and 1992.

be distinguished from SSTs charts. However, nutrient concentrations at 100 m water depth are high along this part of the Indian coast [Conkright *et al.*, 1994]. Even upwelling of low velocity could increase primary productivity in surface waters as indicated by pigment concentrations [Brock *et al.*, 1991; Brock and McClain, 1992]. The high nutrient concentrations could explain higher observed biogenic opal contents in sinking matter obtained from the eastern Arabian Sea compared to the central and western Arabian Sea during periods of similar SSTs. The average SW monsoon total fluxes in the eastern Arabian Sea and their variations are similar to those at the central Arabian Sea station.

4. Conclusion

The intensity of open ocean upwelling and the advection of upwelled water from the Oman coast during the SW monsoon are the main factors controlling the material flux to the interior of the western and, to a lesser extent, the central Arabian Sea. The onset of upwelling occurs between the beginning of May and the beginning of June, which is followed, depending on the rate of cooling of surface water, within 2 to 8 weeks by increasing fluxes. In the western Arabian Sea, highest fluxes were measured during the later phase of the SW monsoon, when the intensification of upwelling favors diatom blooms. These fluxes are higher by a factor of 2 than those in the central Arabian Sea, which is only randomly affected by the diatom blooms. The particle flux in the eastern Arabian Sea is influenced by a separate, weaker upwelling along the Indian coast and almost on the same level as in the central Arabian Sea.

The high fluxes in the western Arabian Sea reveal the most pronounced interannual variability, which is related to variations in the intensity of the Oman upwelling systems and the transport of nutrient-poor south equatorial water to the north. This effect is strongest during high wind speeds which result in low fluxes. Highest fluxes were registered with intermediate wind speeds, suggesting most intense upwelling systems off Oman during moderate SW monsoons.

Acknowledgments. For assistance in deployment and recovery of the sediment trap moorings we thank the mechanical and electronic engineers of the National Institute of Oceanography (Goa) and officers and crew of the research vessels *RV Sagar Kanya* and *RV Sonne*. For providing the MCSST we thank the Physical Oceanographic Distributed Active Archive Center at Jet Propulsion Laboratory, California Institute of Technology. Valuable comments from D. Quadfasel, E. Maier-Reimer, and S. Ewald are acknowledged. We further appreciate the helpful comments and criticisms of I.D. Walsh and an anonymous reviewer. For providing the generic mapping tools (GMT), we thank P. Wessel and W.H.F. Smith. The ongoing sediment trap program is being funded by the German Federal Ministry of Education, Science, Research and Technology (BMBF), the German Research Council (DFG), the Council of Scientific and Industrial Research (CSIR, New Delhi), and the Department of Ocean Development (DOD, New Delhi).

References

- Altered, A.L., and M.W. Silver, Characteristics, dynamics and significance of marine snow, *Prog. Oceanogr.*, 20, 41-82, 1988.
- Anderson, D.M., and W.L. Prell, The structure of the southwest monsoon winds over the Arabian Sea during the Late Quaternary: Observations, simulations, and marine geologic evidence, *J. Geophys. Res.*, 97, 15,481-15,487, 1992.
- Bearmann, G., J. Brown, A. Colling, D. Park, J. Philips, D. Rothery, and J. Wright, *Ocean Circulation*, 238 pp., Open Univ., Milton Keynes, England, 1989.
- Berger, W.H., K. Fisher, C. Lai, and G. Wu, Ocean carbon flux: Global maps of primary production and export production, in *Biogeochemical Cycling and Fluxes Between the Deep Euphotic Zone and Other Oceanic Realms*, edited by C. Agegiani, NOAA Symp. Ser. Undersea Res. NOAA Undersea Res. Program, 3(2), 131-176, 1988.
- Brock, J.C., and C.R. McClain, Interannual variability in phytoplankton blooms observed in the northwestern Arabian Sea during the southwest monsoon, *J. Geophys. Res.*, 97, 733-750, 1992.
- Brock, J.C., C.R. McClain, M.E. Luther, and W.W. Hay, The phytoplankton bloom in the northwest Arabian Sea during the southwest monsoon of 1979, *J. Geophys. Res.*, 96, 20,613-20,622, 1991.
- Brock, J.C., C.R. McClain, and W.W. Hay, A southwest monsoon hydrographic climatology for the northwestern Arabian Sea, *J. Geophys. Res.*, 97, 9455-9465, 1992.
- Brown, O.B., J.G. Bruce, and R.H. Evans, Evolution of sea temperature in the Somali Basin during the southwest monsoon of 1979, *Science*, 209, 595-597, 1980.
- Bruce, J. G., Some details of upwelling of the Somali and Arabian coasts, *J. Mar. Res.*, 32, 419-423, 1974.
- Conkright, M.E., S. Levitus, T.P. Boyer, D.M. Bartolacci, and M.E. Luther, *Atlas of the Northern Indian Ocean*, Natl. Oceanogr. Data Cent., NOAA, Washington, D.C., 1994.
- Curry, W.B., D.R. Ostermann, M.V.S. Guptha, and V. Ittekkot, Foraminiferal production and monsoonal upwelling in the Arabian Sea: Evidence from sediment traps, in *Upwelling Systems: Evolution Since the Early Miocene*, edited by C.P. Summerhayes, W.L. Prell, and K.C. Emeis, *Geol. Soc. Spec. Publ. London*, 64, 93-106, 1992.
- Degens, E.T., and V. Ittekkot, A new look at clay-organic interactions, in *Ein Nord-Süd Profil: Zentraleuropa-Mittelmeerraum-Afrika (Festland Georg Knetsch)*, edited by E.T. Degens, W.E. Krumbain, and A.A. Prashnowsky, *Mitt. Geol. Paläontol. Inst. Univ. Hamburg*, 56, 229-248, 1984.
- Deuser, W.G., and E.H. Ross, Seasonal change in the flux of organic carbon to the deep Sargasso Sea, *Nature*, 283, 364-365, 1980.
- Deuser, W.G., E.H. Ross, and R.R. Anderson, Seasonality in the supply of sediment to the deep Sargasso Sea and implications for the rapid transfer of matter to the deep ocean, *Deep Sea Res., Part A*, 28, 495-505, 1981.
- Dube, S.K., M.E. Luther, and J.J. O'Brien, Relationship between interannual variability in the Arabian Sea and Indian summer monsoon rainfall, *Meteorol. Atmos. Phys.*, 44, 153-165, 1990.
- Düing, W., and A. Leetmaa, Arabian Sea cooling: A preliminary heat budget, *J. Phys. Oceanogr.*, 10, 307-312, 1980.
- Düing, W., R.L. Molinari, and J.C. Swallow, Somali current: Evolution of surface flow, *Science*, 209, 588-590, 1980.
- Dymond, J., and R. Collier, Biogenic particle flux in the equatorial Pacific: Evidence for both high and low productivity during 1982-1993 El Niño, *Global Biogeochem. Cycles*, 2, 129-137, 1988.
- Evans, R.H., and O.B. Brown, Propagation of thermal fronts in the Somali current system, *Deep Sea Res., Part A*, 28, 521-527, 1981.
- Findlater, J., Cross-equatorial jet stream at low level over Kenya, *Meteorol. Mag.*, 95, 353-364, 1966.
- Findlater, J., A major low-level air current near the Indian Ocean during the northern summer, *Q. J. R. Meteorol. Soc.*, 95, 362-380, 1969.
- Fischer, J., F. Schott, and L. Stramma, Currents and transports of the Great Whirl-Socotra Gyre system during the summer monsoon, August 1993, *J. Geophys. Res.*, 101, 3573-3587, 1996.
- Gust, G., R.H. Byrne, R.E. Bernstein, P.R. Betzer, and W. Bowles, Particle fluxes and moving fluids: Experience from synchronous trap collections in the Sargasso Sea, *Deep Sea Res., Part A*, 39, 1071-1083, 1992.
- Gust, G., A.F. Michaels, R. Johnson, W.G. Deuser, and W. Bowles, Mooring line motions and sediment trap hydrodynamics: In situ intercomparison of three common deployment designs, *Deep Sea Res., Part I*, 41, 831-857, 1994.
- Haake, B., T. Rixen and V. Ittekkot, Variability of monsoonal upwelling signals in the deep western Arabian Sea, in *Monsoon Biogeochemistry*, edited by V. Ittekkot and R.R. Nair, *Mitt. Geol. Paläontol. Inst. Univ. Hamburg*, 76, 85-96, 1993a.
- Haake, B., V. Ittekkot, T. Rixen, V. Ramaswamy, R.R. Nair, and W.B. Curry, Seasonality and interannual variability of particle fluxes to the deep Arabian Sea, *Deep Sea Res., Part I*, 40, 1323-1344, 1993b.
- Honjo, S., Seasonality and interaction of biogenic and lithogenic particles flux at the Panama Basin, *Science*, 218, 883-884, 1982.
- Honjo, S., and K.W. Doherty, Large aperture time-series oceanic sediment traps; design objectives, construction, and application, *Deep Sea Res., Part A*, 35, 133-149, 1988.

- Honjo, S., and M.R. Roman, Marine copepod fecal pellets: Production, preservation and sedimentation, *J. Mar. Res.*, **36**, 45-57, 1978.
- Koroleff, F., Determination of silicon, in *Methods of Seawater Analysis*, edited by K. Grasshoff, M. Ehrhardt, and K. Kremling, pp. 174-187, Verlag Chemie, Weinheim, Germany, 1983.
- Lee, C., S.G. Wakeham, and J.I. Hedges, The measurement of particle flux - Are "swimmers" a problem?, *Oceanogr. Mag.*, **1**, 34-36, 1988.
- Lee, C., J.I. Hedges, S.G. Wakeham, and N. Zhu, Effectiveness of various treatments in retarding microbial activity in sediment trap material and their effects on the collection of swimmers, *Limnol. Oceanogr.*, **37**, 117-130, 1992.
- Legler, D.M., I.M. Navon and J.J. O'Brien, Objective analysis of pseudowindstress over the Indian Ocean using a direct minimization approach, *Mon. Weather Rev.*, **117**, 709-720, 1989.
- Luther, M.E., J.J. O'Brien, and W.L. Prell, Variability in upwelling fields in the northwestern Indian Ocean, 1, Model experiments for the last 18,000 years, *Paleoceanography*, **5**, 433-445, 1990.
- McClain, E.P., W.G. Pichel, and C.C. Walton, Comparative performance of AVHRR-based multichannel sea surface temperature, *J. Geophys. Res.*, **90**, 11,587-11,601, 1985.
- McCreary, J.P., Jr., and P.K. Kundu, A numerical investigation of the Somali current during the southwest monsoon, *J. Mar. Res.*, **46**, 25-58, 1988.
- McMillin, L.M., and D.S. Crosby, Theory and validation of multiple window sea surface temperature technique, *J. Geophys. Res.*, **89**, 3655-3661, 1984.
- Molinari, R.L., D.L. Olson, and G. Reverdin, Surface current distribution in the tropical Indian Ocean derived from compilations of surface buoy trajectories, *J. Geophys. Res.*, **95**, 7217-7238, 1990.
- Mortlock, R.A., and P.N. Froelich, A simple method for rapid determination of biogenic opal in pelagic marine sediments, *Deep Sea Res., Part A*, **36**, 1415-1426, 1989.
- Müller, P.J., E. Suess, and A.C. Ungerer, Amino acids and amino sugars of surface particulate and sediment trap material from waters of the Scotia Sea, *Deep Sea Res., Part A*, **33**, 819-838, 1986.
- Nair, R.R., V. Ittekkot, S.J. Manganini, V. Ramaswamy, B. Haake, E.T. Degens, B.N. Desai, and S. Honjo, Increased particle flux to the deep ocean related to monsoons, *Nature*, **338**, 749-751, 1989.
- Qasim, S.Z., Biological productivity of the Indian Ocean, *Indian J. Mar. Sci.*, **6**, 122-137, 1977.
- Ramage, C.S., *Monsoon Meteorology*. 296 pp., Academic, San Diego, Calif., 1971.
- Ramage, C.S., Monsoon climates, in *The Encyclopedia of Climatology*, edited by J.E. Oliver and R.W. Fairbridge, pp. 590-593, Van Nostrand Reinhold, New York, 1987.
- Ryther, J.H., and D.W. Menzel, On the production, composition and distribution of organic matter in the western Arabian Sea, *Deep Sea Res.*, **12**, 199-209, 1965.
- Ryther, J. H., J.R. Hall, A.K. Pease, A. Bakun, and M. Jones, Primary organic production in relation to the chemistry and hydrography of the western Indian Ocean, *Limnol. Oceanogr.*, **11**, 371-380, 1966.
- Sastry, J.S., and R.S. D'Souza, Upwelling and upward mixing in the Arabian Sea, *Indian J. Mar. Sci.*, **1**, 17-27, 1972.
- Schlüssel, P., Passive Fernerkundung der unteren Atmosphäre und der Meeresoberfläche aus dem Weltraum, *Habilitationsschrift Ber. A20*, 175 pp., Zentrum für Meeres- und Klimaforsch. der Univ. Hamburg, Germany, 1995.
- Schott, F., Monsoon response of the Somali current and associated upwelling, *Prog. Oceanogr.*, **12**, 357-383, 1983.
- Schott, F., and M. Fieux, The Somali current in autumn 1984, before the onset of the NE monsoon, *Nature*, **315**, 50-52, 1985.
- Sharma, G.S., Upwelling off the southwest coast of India, *Indian J. Mar. Sci.*, **7**, 209-218, 1978.
- Shetye, S.R., A.D. Gouveia, S.S.C. Shenoi, D. Sundar, G.S. Michael, A.M. Almeida, and K. Sanatanam, Hydrography and circulation off the west coast of India during the southwest monsoon 1987, *J. Mar. Res.*, **48**, 259-378, 1990.
- Smith, W.H.F., and P. Wessel, Gridding with continuous curvature splines in tension, *Geophysics*, **vol. 55**, pp. 293-305, 1990.
- Smetacek, V.S., Role of sinking in diatom life-history cycles: Ecological, evolutionary and geological significance, *Mar. Biol., Berlin*, **84**, 239-251, 1985.
- Smith, S.L., The northwestern Indian Ocean during the monsoons of 1979: Distribution, abundance, and feeding of zooplankton, *Deep Sea Res., Part A*, **29**, 1331-1353, 1982.
- Swallow, J.C., Observation of the Somali current and its relationship to the monsoon winds, in *Monsoon dynamics*, edited by J. Lighthill and R.P. Pearce, pp. 445-451, Cambridge Univ. Press, New York, 1981.
- Tchernia, P., *Descriptive Regional Oceanography*, 2nd ed., 253 pp., Pergamon, Tarrytown, N.Y., 1980.
- Tsai, P.T.H., J.J. O'Brien, and M.E. Luther, The 26-day oscillation observed in the satellite sea surface temperature measurements in the equatorial western Indian Ocean, *J. Geophys. Res.*, **97**, 9605-9618, 1992.
- Wefer, G., Particle flux in the ocean: Effects of episodic production, in *Productivity of the Ocean: Present and Past*, edited by W.H. Berger, V.S. Smetacek, and G. Wefer, pp. 139-154, John Wiley, New York, 1989.
- Wefer, G., and G. Fischer, Seasonal patterns of vertical particle flux in equatorial and coastal upwelling areas of the eastern Atlantic, *Deep Sea Res., Part I*, **40**, 1613-1645, 1993.
- Wefer, G., G. Fischer, D. Fütterer, and R. Gersonde, Seasonal particle flux in the Bransfield Strait, Antarctica, *Deep Sea Res., Part A*, **35**, 891-898, 1988.
- Wessel, P., and W.H.F. Smith, Free software helps map and display data, *EOS Trans. Amer. Geophys. U.*, **vol. 72**, pp. 441, 445-446, 1991.
- Wyrtki, K., Physical oceanography of the Indian Ocean, in *The Biology of the Indian Ocean*, edited by B. Zeitzschel, pp. 18-36, Springer-Verlag, New York, 1973.
- Young, D.K., and J.C. Kindle, Physical processes affecting availability of dissolved silicate for diatom production in the Arabian Sea, *J. Geophys. Res.*, **99**, 22,619-22,632, 1994.

M.V.S. Gupta and R.R. Nair, National Institute of Oceanography, Dona Paula, 403004, Goa, India.

B. Haake, V. Ittekkot, and T. Rixen, Institut für Biogeochemie und Meereschemie, Universität Hamburg, Bundesstr. 55, 20146 Hamburg, Germany. (e-mail: rixen@dkrz.de)

P. Schlüssel, Meteorologisches Institut, Ludwig-Maximilians-Universität München, Theresienstrasse 37, 80333 Munich, Germany.

(Received June 6, 1996; accepted August 5, 1996)